EXTENDED PDF FORMAT
SPONSORED BY
Announcing Enhanced Product Information Pages!
Evaluate our Data. Review Published Results.
Make a Confident Choice.
Learn more
R&D
www.rndsystems.com/PSP

Science
AAAS

Apatite $^4He/^3He$ and (U-Th)/He Evidence for an Ancient Grand Canyon

R. M. Flowers and K. A. Farley

Science **338**, 1616 (2012);
DOI: 10.1126/science.1229390

This copy is for your personal, non-commercial use only.

If you wish to distribute this article to others, you can order high-quality copies for your colleagues, clients, or customers by clicking here.

Permission to republish or repurpose articles or portions of articles can be obtained by following the guidelines here.

The following resources related to this article are available online at www.sciencemag.org (this information is current as of December 21, 2012):

Updated information and services, including high-resolution figures, can be found in the online version of this article at:
http://www.sciencemag.org/content/338/6114/1616.full.html

Supporting Online Material can be found at:
http://www.sciencemag.org/content/suppl/2012/11/28/science.1229390.DC1.html

This article **cites 29 articles**, 14 of which can be accessed free:
http://www.sciencemag.org/content/338/6114/1616.full.html#ref-list-1

Downloaded from www.sciencemag.org on December 21, 2012

Science (print ISSN 0036-8075; online ISSN 1095-9203) is published weekly, except the last week in December, by the American Association for the Advancement of Science, 1200 New York Avenue NW, Washington, DC 20005. Copyright 2012 by the American Association for the Advancement of Science; all rights reserved. The title *Science* is a registered trademark of AAAS.

studies (*14*). The resulting fluid production rate of a few tens of kilograms per second is at the lower end of active volcanic systems that have been proposed to resemble ore-forming systems (*26*). The mechanism of fluid extraction from the magma, however, remains a major unknown in the model. Fluids may accumulate within the chamber beneath an impermeable carapace at the cupola and get episodically ejected together with magma by repeated porphyry-dike injections, which have been observed in many deposits (*1*, *5*, *23*).

In the hydrostatically pressured region above the porphyry ore shell, pulses of magmatic vapor episodically condense into the surrounding fluids and mix in variable proportions. This 100° to 400°C area is at conditions near the boiling curve of saline liquid and switches between a single-phase liquid state (as in Fig. 4A) and a continuous two-phase zone with locally restricted, vapor-dominated fluid lenses rising to the surface. Predicted temperature and pressure conditions are characteristic for acid alteration that overlaps with the tops of some porphyry deposits (*1*) and provide a physical link to epithermal gold mineralization (Fig. 3D) (*27*). These vein deposits often show evidence for episodic boiling events, and gold precipitation is confined to thin layers (*28*), possibly correlating with minor admixing of magmatic fluid pulses in the simulations.

The self-stabilizing process of focused fluid release from large magma chambers also sheds new light on the hydrological dynamics of active volcanoes and sources of geothermal energy. Excess degassing, whereby the amount of released volatiles exceeds the original volatile content of the erupted magma and volcanic conduit, requires fluid focusing from a large degassing magma chamber into a small area of venting (*29*). Quantifying the influence of the brittle-ductile transition on fluid flow is important for the characterization of high-enthalpy geothermal systems (*14*). On the other hand, cooler enhanced geothermal systems are produced through creating permeability by stimulating fluid overpressure, which is similar to vein formation in our porphyry model (*30*). More generally, our study supports the interpretation of permeability as a dynamic parameter that is determined by an intimate interplay of fluid properties, heat advection, and rock mechanics.

References and Notes

1. R. H. Sillitoe, *Econ. Geol.* **105**, 3 (2010).
2. J. W. Hedenquist, J. B. Lowenstern, *Nature* **370**, 519 (1994).
3. R. W. Henley, A. McNabb, *Econ. Geol.* **73**, 1 (1978).
4. J. Arif, T. Baker, *Miner. Depos.* **39**, 523 (2004).
5. J. H. Dilles, *Econ. Geol.* **82**, 1750 (1987).
6. G. Gruen, C. A. Heinrich, K. Schroeder, *Econ. Geol.* **105**, 69 (2010).
7. P. B. Redmond, M. T. Einaudi, E. E. Inan, M. R. Landtwing, C. A. Heinrich, *Geology* **32**, 217 (2004).
8. R. J. Bodnar *et al.*, *Geology* **35**, 791 (2007).
9. M. R. Landtwing *et al.*, *Earth Planet. Sci. Lett.* **235**, 229 (2005).
10. Materials and methods are available as supplementary materials on *Science* Online.
11. S. E. Ingebritsen, C. E. Manning, *Geofluids* **10**, 193 (2010).
12. M. D. Zoback, J. Townend, B. Grollimund, *Int. Geol. Rev.* **44**, 383 (2002).
13. R. O. Fournier, *Econ. Geol.* **94**, 1193 (1999).
14. D. O. Hayba, S. E. Ingebritsen, *J. Geophys. Res.* **102**, (B6), 12235 (1997).
15. S. F. Cox, *Geofluids* **10**, 217 (2010).
16. L. M. Cathles, *Econ. Geol.* **88**, 1977 (1993).
17. D. Coumou, T. Driesner, C. A. Heinrich, *Science* **321**, 1825 (2008).
18. T. Jupp, A. Schultz, *Nature* **403**, 880 (2000).
19. S. A. Rojstaczer, S. E. Ingebritsen, D. O. Hayba, *Geofluids* **8**, 128 (2008).
20. B. G. Rusk, M. H. Reed, *Geology* **30**, 727 (2002).
21. P. L. Cloke, S. E. Kesler, *Econ. Geol.* **74**, 1823 (1979).
22. A. Hezarkhani, A. E. Williams-Jones, C. H. Gammons, *Miner. Depos.* **34**, 770 (1999).
23. J. M. Proffett, *Econ. Geol.* **98**, 1535 (2003).
24. L. M. Cathles, R. Shannon, *Earth Planet. Sci. Lett.* **262**, 92 (2007).
25. A. von Quadt *et al.*, *Geology* **39**, 731 (2011).
26. J. W. Hedenquist, M. Aoki, H. Shinohara, *Geology* **22**, 585 (1994).
27. R. W. Henley, A. J. Ellis, *Earth Sci. Rev.* **19**, 1 (1983).
28. E. Izawa *et al.*, *J. Geochem. Explor.* **36**, 1 (1990).
29. H. Shinohara, *Rev. Geophys.* **46**, RG4005 (2008).
30. K. F. Evans, A. Genter, J. Sausse, *J. Geophys. Res.* **110**, B04204 (2005).

Acknowledgments: This work was supported by the Swiss National Science Foundation. We thank the reviewers for inspiring thoughts on the manuscript. This study benefited from discussions with D. Coumou, S. Cox, J. Dilles, S. Geiger, S. Matthai, and many others. Selected data and code are provided as supplementary materials.

Supplementary Materials

www.sciencemag.org/cgi/content/full/science.1225009/DC1
Materials and Methods
Figs. S1 to S3
References and Notes (*31–52*)
Movies S1 and S2
Database S1

21 May 2012; accepted 26 October 2012
Published online 15 November 2012;
10.1126/science.1225009

Apatite $^4He/^3He$ and (U-Th)/He Evidence for an Ancient Grand Canyon

R. M. Flowers[1]* and K. A. Farley[2]

The Grand Canyon is one of the most dramatic features on Earth, yet when and why it was carved have been controversial topics for more than 150 years. Here, we present apatite $^4He/^3He$ thermochronometry data from the Grand Canyon basement that tightly constrain the near-surface cooling history associated with canyon incision. $^4He/^3He$ spectra for eastern Grand Canyon apatites of differing He date, radiation damage, and U-Th zonation yield a self-consistent cooling history that substantially validates the He diffusion kinetic model applied here. Similar data for the western Grand Canyon provide evidence that it was excavated to within a few hundred meters of modern depths by ~70 million years ago (Ma), in contrast to the conventional model in which the entire canyon was carved since 5 to 6 Ma.

The very existence of the Grand Canyon (Arizona, United States) (Fig. 1) inspires questions about why rivers sometimes carve canyons, how drainage systems and landscapes evolve, and how these processes relate to continental elevation gain. The prevailing view is that canyon carving occurred after 5 to 6 million years ago (Ma), when detritus derived from the upstream reaches of the Colorado River system first appeared in Grand Wash Trough at the river's western exit from the Colorado Plateau (*1–3*). Many consider the absence of such diagnostic deposits before 6 Ma as evidence that the Grand Canyon was not yet excavated (*4*, *5*), with most recent debate focused on how river integration occurred (*5–7*). This interpretation assumes that establishment of the integrated Colorado River drainage requires coeval canyon carving.

However, a puzzling array of data hints that the canyon's origin is more complex and could predate integration. Direct geochronologic constraints demanding post–6 Ma formation of the entire canyon do not exist. Dated volcanic rocks drape the western Grand Canyon ≤75 m above modern river level (*8*), constraining only the most recent ~8% of the total ~1000 m of canyon incision at this location. For the eastern canyon, dated basalts, travertines, and alluvium are ≤0.5 Ma and <200 m above river level (*4*, *9–11*) and resolve <20% of total incision. Speleothem dates may extend this record (*12*), but their interpretation as incision constraints is debated because it relies on unproven paleohydraulic assumptions (*4*, *13*). A western canyon speleothem date 290 m above river level suggests that the lower ~30% of western canyon carving occurred after ~3.9 Ma (*12*). Thus, the upper ~70% of the western Grand Canyon lacks any direct geochronologic constraint on when it was carved. In the eastern part of the canyon, 2.19- to 3.72-Ma speleothems located ~900 m above the river (*12*) imply that the majority of the 1500 m

[1]Department of Geological Sciences, University of Colorado at Boulder, 2200 Colorado Avenue, UCB 399, Boulder, CO 80309, USA. [2]Division of Geological and Planetary Sciences, California Institute of Technology, MS 170-25, Pasadena, CA 91125, USA.

*To whom correspondence should be addressed. E-mail: rebecca.flowers@colorado.edu

Downloaded from www.sciencemag.org on December 21, 2012

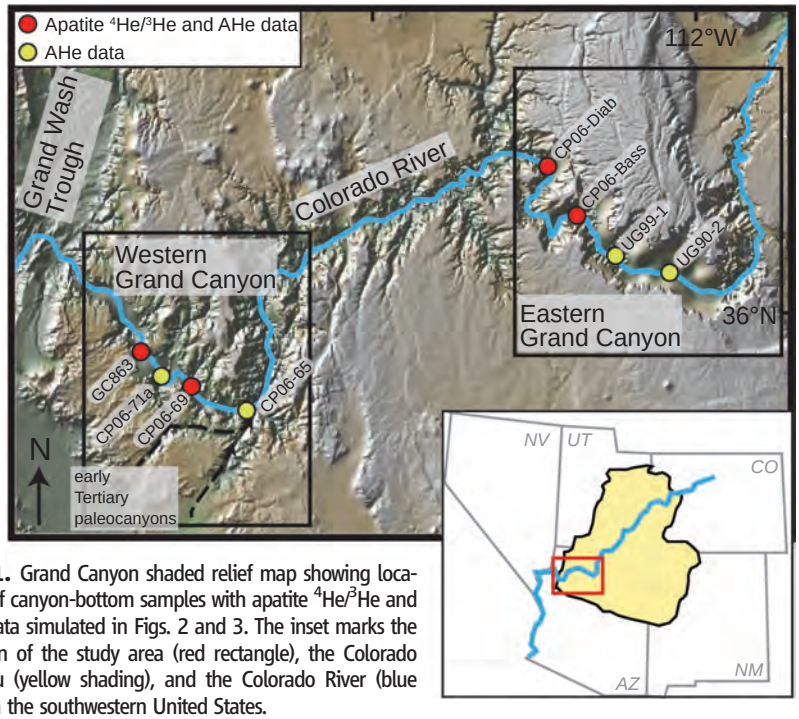

Fig. 1. Grand Canyon shaded relief map showing locations of canyon-bottom samples with apatite ^{4}He/^{3}He and AHe data simulated in Figs. 2 and 3. The inset marks the location of the study area (red rectangle), the Colorado Plateau (yellow shading), and the Colorado River (blue line) in the southwestern United States.

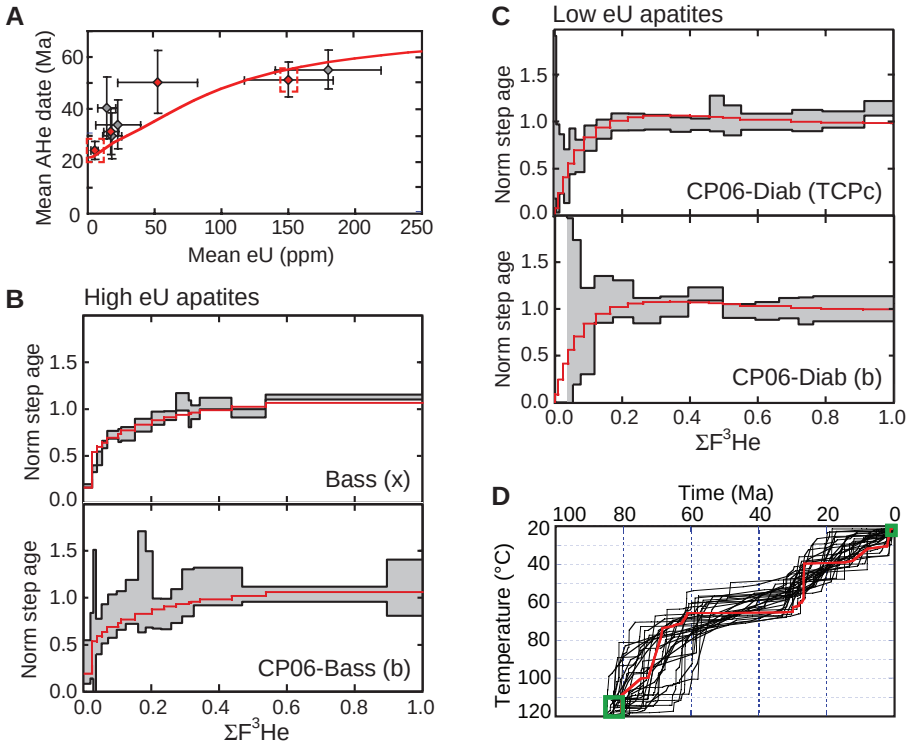

Fig. 2. Results for the eastern Grand Canyon. (**A**) Mean sample AHe date versus mean apatite eU for eight samples (errors at ±1σ SD). Dashed red boxes mark the two samples with apatite ^{4}He/^{3}He data. Samples with apatite U-Th zonation data are indicated with diamonds, with their AHe dates corrected for α ejection using the mean FTZ (*26*) values of grains with U-Th zonation data. The red curve shows the predicted date-eU correlation from best-fit thermal history in (D). ppm, parts per million. Normalized ^{4}He/^{3}He step age plots for (**B**) two high eU apatites and (**C**) two low eU apatites, with 1σ uncertainties. Red curves are profiles predicted by best-fit thermal history in (D). ΣF^{3}He, cumulative ^{3}He release fraction. (**D**) Thermal histories that satisfy the AHe dates for the four samples of variable eU marked by red diamonds in (A) [goodness-of-fit parameter $G = 0.3$ (*30*)] and the four normalized step age profiles in (B) and (C) ($G = 0.15$). The red line denotes best-fit thermal history. Green boxes are thermal history constraints. Although we have AHe data for eight eastern canyon–bottom samples (*23*), for clarity only the locations of the four simulated samples are shown in Fig. 1.

of incision at this site occurred after 6 Ma, again subject to paleo-groundwater table assumptions.

Other observations imply an older origin for at least parts of the canyon. Deeply incised paleochannels on the Colorado Plateau's southwestern edge support an extensive northeastward-flowing paleodrainage system that included portions of a paleo–Grand Canyon in the early Tertiary (*14*–*17*). Substantial canyon incision between 17 and 6 Ma was inferred from 19-Ma lavas on the plateau surface (*15*, *18*, *19*) and from speleothem dates (*12*), but the latter are controversial, owing to their distal locations from the canyon (*13*, *20*). If an older canyon existed, it is possible that a smaller drainage basin in largely carbonate lithologies explains the absence of pre–6 Ma Colorado River clastics in the Grand Wash Trough (*19*, *21*). Grand Canyon history is further complicated by the possibility that its eastern and western segments evolved independently and later merged into the modern configuration (*15*). As discussed below, our work supports an east-west dichotomy in incision history, and our data are presented accordingly.

Apatite (U-Th)/He (AHe) thermochronometry can document canyon incision because of its unique sensitivity to topographically induced temperature variations in the shallow crust (*22*). Rocks cool as they approach Earth's surface by erosion, and AHe data record this cooling history. Prior application of this method to the eastern Grand Canyon suggested incision of a kilometer-scale paleocanyon by 55 Ma, with subsequent downcutting of this canyon below the modern plateau surface in late Tertiary time. This history is compatible with the suggestion that incision of much of the eastern half of the canyon occurred after 6 Ma (*23*). In contrast, AHe data from the western Grand Canyon suggest excavation to within several hundred meters of the canyon's modern depth by ~70 Ma, in direct conflict with the young canyon model (*21*). The unexpected implications of this initial Grand Canyon AHe work motivated the apatite ^{4}He/^{3}He and U-Th zonation study presented here.

The apatite ^{4}He/^{3}He method provides even greater sensitivity to canyon incision by constraining cooling histories down to ~30°C from the spatial distribution of radiogenic ^{4}He in the crystal (*24*). Successful interpretation of both AHe dates and ^{4}He/^{3}He spectra demands accurate understanding of He behavior in apatite. Although the role of radiation damage in retarding apatite He diffusion and the superposition of U-Th zonation effects on ^{4}He/^{3}He spectra have recently been characterized (*25*–*28*), verification of the methodology is limited. Because the eastern Grand Canyon yields AHe dates that are generally consistent with previous models of late Tertiary canyon incision, we use this region as a test case for the ^{4}He/^{3}He method. With the use of a recent He diffusion kinetic model (*28*), our goal is to assess whether the ^{4}He/^{3}He results from this suite—which includes apatites of variable He date, degree of radiation damage,

Downloaded from www.sciencemag.org on December 21, 2012

and U-Th zonation—yield mutually consistent thermal histories. Fulfillment of this expectation validates application of the method to a similar data set from the western Grand Canyon to test the "young" versus "ancient" canyon models.

From two eastern canyon–bottom samples, we acquired $^4He/^3He$ spectra on apatites that have a large difference in effective uranium concentration (eU) (*29*) and mean AHe date (Fig. 2, fig. S1, and tables S1 and S2). We selected these two samples from a suite in which He dates are correlated with eU, diagnostic of the effects of radiation damage on He diffusivity (*23*) (Fig. 2A). We mapped U and Th concentrations in these apatites plus those from two other samples in the suite (fig. S2 and tables S3 and S4). We performed inverse modeling to find time-temperature paths that simultaneously satisfy the mean AHe dates and the $^4He/^3He$ spectra (*30*) (table S5).

Thermal histories were forced through 110° to 120°C peak temperatures at 80 to 85 Ma, as suggested by complete annealing of apatite fission tracks at this time (*31*), and cooling to 20° to 25°C surface temperature by present-day. Statistically acceptable paths (*30*) are characterized by a distinctive two-stage cooling trajectory, impose tight constraints on the ~90° to 30°C thermal history experienced by the eastern gorge, and are consistent with but more restrictive than the history inferred from the AHe dates alone (*28*) and apatite fission-track (AFT) data from the same area (Fig. 2D) (*32*). This history records a distinct late Tertiary cooling phase, permissive of substantial post–6 Ma incision. Importantly, the agreement among samples with differing eU provides compelling evidence that the He diffusion kinetic model we used is appropriate for simulation of Grand Canyon AHe and $^4He/^3He$ data.

Given this validation, we examined a similar suite of data from the western Grand Canyon (Fig. 1). Late Cretaceous AHe dates for four canyon-bottom samples (*23*, *26*) show no correlation with apatite eU, consistent with a single-phase cooling history also indicated by AFT data (*32*) (tables S1 and S6). Apatite $^4He/^3He$ data were obtained from two of these samples (Fig. 3, fig. S1, and tables S1 and S2). Duplicate $^4He/^3He$ spectra for one sample (CP06-69) are similar, and apatites from this sample are characterized by similar U-Th zonation (fig. S2 and tables S3 and S4). In contrast, the 11 apatite $^4He/^3He$ spectra for sample GC863 have diverse shapes, arising from extreme U-Th zoning heterogeneity in this sample (*26*) (figs. S1 and S2). Because we do not have U-Th zonation data for each apatite with $^4He/^3He$ data, this extreme zonation precludes the use of the GC863 $^4He/^3He$ results for inverse modeling.

Consequently, we used the $^4He/^3He$ spectra from CP06-69 and the AHe dates from all four basement samples (table S5) to constrain statistically acceptable thermal histories for the western Grand Canyon (*30*). We used the same thermal history constraints as for the eastern Grand Canyon, differing only in broader age bounds of 100 to 80 Ma for the peak temperature, owing to the older AHe dates here. Statistically acceptable paths (*30*) require rapid cooling to <30°C by ~70 Ma (Fig. 3). Assuming a 20-to-25°C/km geothermal gradient and a 25°C surface temperature (*21*, *30*), this result implies carving of the western Grand Canyon to within several hundred meters of modern depths (70 to 80% of total incision) by 70 Ma. This history is compatible with the volcanic and speleothem data within the western gorge (*8*, *12*).

We used a time-temperature path constructed from a popular description of post–6 Ma incision (*4*, *30*) to explicitly test the young canyon model against our western canyon $^4He/^3He$ spectra and bulk AHe dates. The predicted distribution of AHe dates is much broader and includes dates younger than observed (Fig. 3). Similarly, the fits of the predicted $^4He/^3He$ spectra to the measurements are statistically unacceptable (Fig. 3B). These conclusions are insensitive to reasonable assumptions about the geotherm and surface temperature and to alternative diffusivity parameters (*30*) (fig. S3A). The young canyon model also yields a qualitatively poorer fit than the ancient canyon model to the $^4He/^3He$ spectra of the strongly eU-zoned sample GC863 (*30*) (fig. S3B).

The western Grand Canyon $^4He/^3He$ and AHe data demand a substantial cooling event at 70 to 80 Ma and provide no evidence for the strong post–6 Ma cooling signal predicted by the young canyon model. Thus, when applying our best understanding of apatite He diffusion kinetics derived from recent work (*25*, *28*), apatite He data support carving of most of the western Grand Canyon by ~70 Ma and are inconsistent with the conventional view that the entire canyon was cut after 6 Ma (*4*). Moreover, the results imply a dichotomy in eastern and western canyon carving, characterized by coeval excavation of an eastern paleocanyon (*23*) and substantial carving of the modern western gorge by 70 Ma (*21*), followed by substantial late Tertiary incision restricted to the eastern canyon. This history supports a model (*21*) in which much of the Grand Canyon was carved by an ancient Cretaceous river that flowed eastward from western highlands, with Tertiary reversal of the river's course as topography rose in the east and collapsed in the west. Thus, this incision history has profound implications for the evolution of topography, landscapes, hydrology, and tectonism in the North American Cordillera.

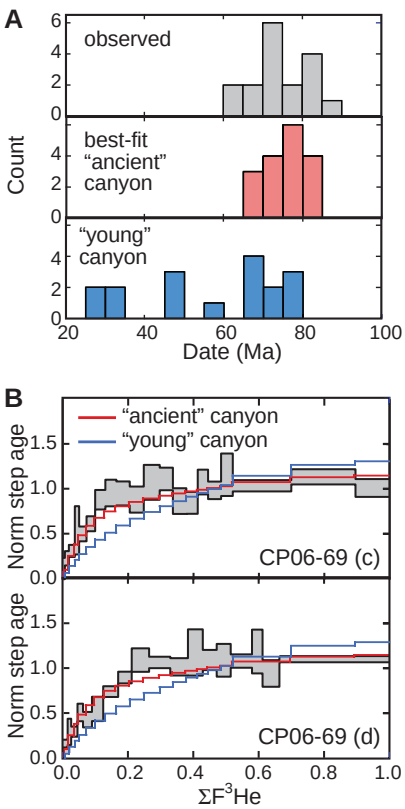

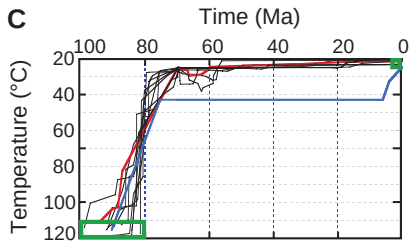

Fig. 3. Results for the western Grand Canyon. (**A**) Distribution of measured AHe dates for multiple replicates of four samples (upper panel) compared with AHe dates predicted by the best-fit thermal history from the inverse modeling suggesting an "ancient" Late Cretaceous canyon [middle histogram, using the red cooling path in (C)], and those predicted by the conventional "young" post–6 Ma canyon model [bottom histogram, using the blue path in (C)]. (**B**) Normalized $^4He/^3He$ step age plots for two apatites from CP06-69. Red and blue curves are profiles predicted by the best-fit and young canyon thermal histories in (C), respectively. (**C**) Thermal histories that satisfy the bulk AHe data in (A) ($G = 0.3$) and the two normalized step age profiles in (B) ($G = 0.32$). The red line denotes best-fit thermal history. The blue line shows conventional post–6 Ma incision history based on (*4*) as described in (*30*) and yields a substantially poorer fit to the AHe data and $^4He/^3He$ spectra in (A) and (B) ($G < 0.06$). Green boxes are thermal history constraints.

References and Notes

1. E. Blackwelder, *Geol. Soc. Am. Bull.* **45**, 551 (1934).
2. C. R. Longwell, *Am. J. Sci.* **244**, 817 (1946).
3. I. Lucchitta, *Geol. Soc. Am. Bull.* **83**, 1933 (1972).
4. K. E. Karlstrom, R. Crow, L. J. Crossey, D. Coblentz, J. W. Van Wijk, *Geology* **36**, 835 (2008).
5. J. L. Pederson, *GSA Today* **18**, 4 (2008).
6. J. E. Spencer, P. A. Pearthree, in *Colorado River Origin and Evolution*, R. A. Young, E. E. Spamer, Eds. (Grand Canyon Association, Grand Canyon, AZ, 2001), pp. 215–222.
7. I. Lucchitta, R. F. Holm, B. K. Lucchitta, *GSA Today* **21**, 4 (2011).
8. K. E. Karlstrom *et al.*, *Geol. Soc. Am. Bull.* **119**, 1283 (2007).
9. J. Pederson, K. Karlstrom, W. Sharp, W. McIntosh, *Geology* **30**, 739 (2002).
10. S. W. Davis *et al.*, in *Colorado River Origin and Evolution*, R. A. Young, E. E. Spamer, Eds. (Grand Canyon Association, Grand Canyon, AZ, 2001), pp. 135–139.

Downloaded from www.sciencemag.org on December 21, 2012

11. I. Lucchitta, G. H. Curtis, M. E. Davis, S. W. Davis, B. Turrin, *Quat. Res.* **53**, 23 (2000).
12. V. Polyak, C. Hill, Y. Asmerom, *Science* **319**, 1377 (2008).
13. J. Pederson, R. Young, I. Lucchitta, L. S. Beard, G. Billingsley, *Science* **321**, 1634b (2008).
14. R. A. Young, *Tectonophysics* **61**, 25 (1979).
15. D. P. Elston, R. A. Young, *J. Geophys. Res.* **96**, 12389 (1991).
16. A. R. Potochnik, in *Colorado River Origin and Evolution*, R. A. Young, E. E. Spamer, Eds. (Grand Canyon Association, Grand Canyon, AZ, 2001), pp. 17–22.
17. R. A. Young, in *Colorado River Origin and Evolution*, R. A. Young, E. E. Spamer, Eds. (Grand Canyon Association, Grand Canyon, AZ, 2001), pp. 7–16.
18. R. A. Young, in *Geology of Grand Canyon, Northern Arizona*, D. P. Elston, G. H. Billingsley, R. A. Young, Eds. (28th International Geological Congress Fieldtrip Guidebook T115/315, American Geophysical Union, Washington, DC, 1989), pp. 166–173.
19. R. A. Young, in *Late Cenozoic Drainage History of the Southwestern Great Basin and Lower Colorado River Basin: Geologic and Biologic Perspectives*, M. C. Reheis, R. Hershler, D. M. Miller, Eds. (Geological Society of America Special Paper, Geological Society of America, Boulder, CO, 2008), vol. 439, pp. 319–333.
20. P. A. Pearthree, J. E. Spencer, J. E. Faulds, P. K. House, *Science* **321**, 1634 (2008).
21. B. Wernicke, *Geol. Soc. Am. Bull.* **123**, 1288 (2011).
22. M. A. House, B. P. Wernicke, K. A. Farley, *Nature* **396**, 66 (1998).
23. R. M. Flowers, B. P. Wernicke, K. A. Farley, *Geol. Soc. Am. Bull.* **120**, 571 (2008).
24. D. L. Shuster, K. A. Farley, *Earth Planet. Sci. Lett.* **217**, 1 (2004).
25. K. A. Farley, D. L. Shuster, E. B. Watson, K. H. Wanser, G. Balco, *Geochem. Geophys. Geosyst.* **11**, Q10001 (2010).
26. K. A. Farley, D. L. Shuster, R. A. Ketcham, *Geochim. Cosmochim. Acta* **75**, 4515 (2011).
27. D. L. Shuster, R. M. Flowers, K. A. Farley, *Earth Planet. Sci. Lett.* **249**, 148 (2006).
28. R. M. Flowers, R. A. Ketcham, D. L. Shuster, K. A. Farley, *Geochim. Cosmochim. Acta* **73**, 2347 (2009).
29. R. M. Flowers, D. L. Shuster, B. P. Wernicke, K. A. Farley, *Geology* **35**, 447 (2007).
30. Materials and methods are available as supplementary materials on *Science* Online.
31. T. A. Dumitru, I. R. Duddy, P. F. Green, *Geology* **22**, 499 (1994).
32. S. A. Kelley, C. E. Chapin, K. Karlstrom, in *Colorado River Origin and Evolution*, R. A. Young, E. E. Spamer, Eds. (Grand Canyon Association, Grand Canyon, AZ, 2001), pp. 37–42.

Acknowledgments: This work was supported by NSF grant EAR-1019896 to K.A.F. The data reported in this paper are tabulated in the supplementary materials. We thank B. Wernicke for discussion.

Supplementary Materials

www.sciencemag.org/cgi/content/full/science.1229390/DC1
Materials and Methods
Figs. S1 to S3
Tables S1 to S6
References (*33–40*)

27 August 2012; accepted 7 November 2012
Published online 29 November 2012;
10.1126/science.1229390

Multiplex Targeted Sequencing Identifies Recurrently Mutated Genes in Autism Spectrum Disorders

Brian J. O'Roak,[1] Laura Vives,[1] Wenqing Fu,[1] Jarrett D. Egertson,[1] Ian B. Stanaway,[1] Ian G. Phelps,[2,3] Gemma Carvill,[2,3] Akash Kumar,[1] Choli Lee,[1] Katy Ankenman,[4] Jeff Munson,[4] Joseph B. Hiatt,[1] Emily H. Turner,[1] Roie Levy,[1] Diana R. O'Day,[2] Niklas Krumm,[1] Bradley P. Coe,[1] Beth K. Martin,[1] Elhanan Borenstein,[1,5,6] Deborah A. Nickerson,[1] Heather C. Mefford,[2,3] Dan Doherty,[2,3] Joshua M. Akey,[1] Raphael Bernier,[4] Evan E. Eichler,[1,7]* Jay Shendure[1]*

Exome sequencing studies of autism spectrum disorders (ASDs) have identified many de novo mutations but few recurrently disrupted genes. We therefore developed a modified molecular inversion probe method enabling ultra-low-cost candidate gene resequencing in very large cohorts. To demonstrate the power of this approach, we captured and sequenced 44 candidate genes in 2446 ASD probands. We discovered 27 de novo events in 16 genes, 59% of which are predicted to truncate proteins or disrupt splicing. We estimate that recurrent disruptive mutations in six genes—*CHD8*, *DYRK1A*, *GRIN2B*, *TBR1*, *PTEN*, and *TBL1XR1*—may contribute to 1% of sporadic ASDs. Our data support associations between specific genes and reciprocal subphenotypes (*CHD8*-macrocephaly and *DYRK1A*-microcephaly) and replicate the importance of a β-catenin–chromatin-remodeling network to ASD etiology.

There is considerable interest in the contribution of rare variants and de novo mutations to the genetic basis of complex phenotypes such as autism spectrum disorders (ASDs). However, because of extreme genetic heterogeneity, the sample sizes required to implicate any single gene in a complex phenotype are extremely large (*1*). Exome sequencing has identified hundreds of ASD candidate genes on the basis of de novo mutations observed in the affected offspring of unaffected parents (*2–6*). Yet, only a single mutation was observed in nearly all such genes, and sequencing of over 900 trios was insufficient to establish mutations at any single gene as definitive genetic risk factors (*2–6*).

To address this, we sought to evaluate candidate genes identified by exome sequencing (*2*, *3*) for de novo mutations in a much larger ASD cohort. We developed a modified molecular inversion probe (MIP) strategy (Fig. 1A) (*7–9*) with novel algorithms for MIP design; an optimized, automatable work flow with robust performance and minimal DNA input; extensive multiplexing of samples while sequencing; and reagent costs of less than $1 per gene per sample. Extensive validation using several probe sets and sample collections demonstrated 99% sensitivity and 98% positive predictive value for single-nucleotide variants at well-covered positions, i.e., 92 to 98% of targeted bases (figs. S1 to S7 and tables S1 to S9) (*10*).

We applied this method to 2494 ASD probands from the Simons Simplex Collection (SSC) (*11*) using two probe sets [ASD1 (6 genes) and ASD2 (38 genes)] to target 44 ASD candidate genes (*12*). Preliminary results using ASD1 on a subset of the SSC implicated *GRIN2B* as a risk locus (*3*). The 44 genes were selected from 192 candidates (*2*, *3*) by focusing on genes with disruptive mutations, associations with syndromic autism (*13*), overlap with known or suspected neurodevelopmental copy number variation (CNV) risk loci (*13*, *14*), structural similarities, and/or neuronal expression (table S3). Although a few of the 44 genes have been reported to be disrupted in individuals with neurodevelopmental or neuropsychiatric disorders (often including concurrent dysmorphologies), their role in so-called idiopathic ASDs has not been rigorously established. Twenty-three of the 44 genes intersect a 49-member β-catenin–chromatin-remodeling protein-protein interaction (PPI) network (*2*) or an expanded 74-member network (figs. S8 and S9) (*3*, *4*).

We required samples to successfully capture with both probe sets, yielding 2446 ASD probands with MIP data, 2364 of which had only MIP data and for 82 of which we had also sequenced their exomes (*2*, *3*). The high GC content of several candidates required considerable rebalancing to improve capture uniformity (*12*) (figs. S3A and S10). Nevertheless, the reproducible behavior of most MIPs allowed us to identify copy number variation at targeted genes, including several inherited duplications (figs. S11 and S12 and table S10).

To discover de novo mutations, we first identified candidate sites by filtering against variants observed in other cohorts, including non-ASD exomes and MIP-based resequencing of 762 healthy, non-ASD individuals (*12*). The remaining

[1]Department of Genome Sciences, University of Washington School of Medicine, Seattle, WA 98195, USA. [2]Department of Pediatrics, University of Washington School of Medicine, Seattle, WA 98195, USA. [3]Seattle Children's Hospital, Seattle, WA 98105, USA. [4]Department of Psychiatry and Behavioral Sciences, University of Washington, Seattle, WA 98195, USA. [5]Department of Computer Science and Engineering, University of Washington, Seattle, WA 98195, USA. [6]Santa Fe Institute, Santa Fe, NM 87501, USA. [7]Howard Hughes Medical Institute, Seattle, WA 98195, USA.

*To whom correspondence should be addressed. E-mail: shendure@uw.edu (J.S.); eee@gs.washington.edu (E.E.E.)

Downloaded from www.sciencemag.org on December 21, 2012